

# The role of glycinergic inhibition in respiratory pattern formation and cardio-respiratory coupling in rats



Werner Issao Furuya, Rishi R. Dhingra, Pedro Trevizan-Baú, Robin M. McAllen, Mathias Dutschmann\*

The Florey Institute of Neuroscience and Mental Health, 30 Royal Parade, Parkville, Victoria, Australia

## ARTICLE INFO

### Keywords:

Respiratory pattern  
Fast synaptic inhibition  
Cardio-respiratory  
Cardiac vagal tone  
Pre-motor circuit

## ABSTRACT

Cardio-respiratory coupling is reflected as respiratory sinus arrhythmia (RSA) and inspiratory-related bursting of sympathetic nerve activity. Inspiratory-related inhibitory and/or postinspiratory-related excitatory drive of cardiac vagal motoneurons (CVMs) can generate RSA. Since respiratory oscillations may depend on synaptic inhibition, we investigated the effects of blocking glycinergic neurotransmission (systemic and local application of the glycine receptor (GlyR) antagonist, strychnine) on the expression of the respiratory motor pattern, RSA and sympatho-respiratory coupling. We recorded heart-rate, phrenic, recurrent laryngeal and thoracic sympathetic nerve activities (PNA, RLNA, t-SNA) in a working-heart-brainstem preparation of rats, and show that systemic strychnine (50–200 nM) abolished RSA and triggered a shift of postinspiratory RLNA into inspiration, while t-SNA remained unchanged. Bilateral strychnine microinjection into the ventrolateral medullary area containing CVMs and laryngeal motoneurons (LMNs) of the nucleus ambiguus (NA/CVLM), the nucleus tractus solitarius, pre-Bötzinger Complex, Bötzinger Complex or Kölliker-Fuse nuclei revealed that only NA/CVLM strychnine microinjections mimicked the effects of systemic application. In all other target nuclei, except the Bötzinger Complex, GlyR-blockade attenuated the inspiratory-tachycardia of the RSA to a similar degree while evoking only a modest change in respiratory motor patterning, without changing the timing of postinspiratory-RLNA, or t-SNA. Thus, glycinergic inhibition at the motoneuronal level is involved in the generation of RSA and the separation of inspiratory and postinspiratory bursting of LMNs. Within the distributed ponto-medullary respiratory pre-motor network, local glycinergic inhibition contribute to the modulation of RSA tachycardia, respiratory frequency and phase duration but, surprisingly it had no major role in the mediation of respiratory-sympathetic coupling.

## 1. Introduction

Respiration and cardiovascular function are coupled and such coupling can be observed as respiratory modulation of heart rate (HR) known as respiratory sinus arrhythmia (RSA) and respiratory bursting of sympathetic motor outputs (Richter and Spyer, 1990). Oscillation between inspiratory-related inhibition (Gilbey et al., 1984; Iriuchijima and Kumada, 1964; Kunze, 1972; McAllen and Spyer, 1978) and postinspiratory-related excitatory drive (Farmer et al., 2016) of cardiac vagal motor neurons (CVMs) is seen as the primary synaptic mechanism that generates RSA. Sympatho-respiratory coupling is observed as an inspiratory burst of sympathetic activity that can be recorded on sympathetic nerves *in situ* and *in vivo* (Adrian et al., 1932; Dick et al., 2004; Gilbey, 2007; Pickering and Paton, 2006; Pilowsky, 1995).

Recently, we have demonstrated that balanced excitation and

inhibition within the ventrolateral respiratory column, dorsal respiratory group and pontine respiratory group is necessary for the expression of the three-phase respiratory motor pattern (Dhingra et al., 2019a). Further, by mapping the distribution of local field potentials throughout a broad region of the medulla and pons that contain the core elements of the respiratory network, we were able to demonstrate that the transition from inspiration to postinspiration simultaneously engaged an expansive network that includes the ventrolateral respiratory column, dorsal and pontine respiratory groups (Dhingra et al., 2020). Further, the formation of the respiratory motor pattern depends on synaptic interactions between the medullary ventrolateral respiratory column and the pontine respiratory groups (Jones and Dutschmann, 2016). More specifically, the integrity of the pontine Kölliker-Fuse nuclei (KF<sub>n</sub>) is essential for gating cranial nerve motor outputs and postinspiratory network activity and for the timing of the inspiratory-postinspiratory phase transition

\* Corresponding author.

E-mail address: [mathias.dutschmann@florey.edu.au](mailto:mathias.dutschmann@florey.edu.au) (M. Dutschmann).

<https://doi.org/10.1016/j.crphys.2021.03.001>

Received 27 October 2020; Received in revised form 11 February 2021; Accepted 12 March 2021

2665-9441/© 2021 The Author(s). Published by Elsevier B.V. This is an open access article under the CC BY-NC-ND license (<http://creativecommons.org/licenses/by-nc-nd/4.0/>).

(Dutschmann and Herbert, 2006; Dutschmann et al., 2021). Given the reflection of the inspiratory to postinspiratory phase transition in cardio-respiratory motor patterns, it is not surprising that previous publications have shown that ponto-medullary transection abolishes the RSA and the sympatho-respiratory coupling (Baekey et al., 2008). Further, specific local inhibition of the KFn abolishes tonic and post-inspiratory excitatory premotor drive to the CVMs that, consequently, abolishes the postinspiratory bradycardia of RSA (Farmer et al., 2016). A recent publication showed that optogenetic manipulation of inspiratory rhythm generating circuit of the pre-Böttinger complex (pre-BötC) also exerts profound effects on the expression of RSA and sympatho-respiratory coupling (Menuet et al., 2020). Additional anatomical and functional evidence is supporting the view that cardio-respiratory interactions are mediated by a distributed network. For instance, transneuronal labelling of the network driving the stellate ganglion, the principal source of sympathetic activity driving the heart, identified a distributed population of interneurons within the hypothalamus, pons, medulla and spinal cord (Jansen et al., 1995).

Given that cardio-respiratory modulation strongly reflects the inspiratory-postinspiratory oscillation of reciprocally connected inspiratory and postinspiratory neurons (Richter, 1982; Rybak et al., 2004, 2007; Smith et al., 2007; Abdala et al., 2009; Shevtsova et al., 2014; Marchenko et al., 2016) neurons, we hypothesized that fast synaptic inhibition neurotransmission is not only required for the formation of the sequential three-phase respiratory motor activity, but may also contribute to generation of RSA and the coupling of respiratory and sympathetic motor activities.

A glycine is a prominent fast inhibitory neurotransmitter and glycine receptors (GlyR) and glycinergic neurons, are found throughout the brainstem and spinal cord and are specifically located within known cardio-respiratory areas (Manzke et al., 2010; Zafra et al., 1995). Glycinergic neurotransmission has been shown to play important roles in the regulation of central respiratory activity (Hayashi and Lipski 1992; Gomeza et al., 2003; Bonngiani et al., 2010; Manzke et al., 2010; Richter and Smith, 2014). In particular, systemic antagonism of glycinergic neurotransmission was reported to cause a shift of the onset of post-inspiratory motor bursting from early expiration to inspiration and therefore a prominent role for the timely mediation of inspiratory-postinspiratory phase oscillations (Busselberg et al., 2001a, 2001b, 2003; Dutschmann & Paton, 2002a, 2002b, 2002c; Ezure et al., 2003; Shevtsova et al., 2014). Taken together, we hypothesize that glycinergic inhibition plays an important role in the mediation of RSA and sympatho-respiratory motor coupling.

To test this hypothesis, we compared the effects of systemic and local blockade of GlyRs with the GlyR antagonist strychnine on the formation of the respiratory motor pattern, RSA and sympatho-respiratory coupling from simultaneous recordings of HR, phrenic, recurrent laryngeal and thoracic sympathetic nerve activities (PNA, RLNA, t-SNA) in the *in situ* working heart-brainstem preparation of rats.

## 2. Methods

### 2.1. Animals

Juvenile Sprague-Dawley rats of either sex (post-natal day 15–26, weighing 40–70 g) were used (n = 47). Animals were maintained on a 12-h light/dark cycle with laboratory chow and water available *ad libitum*. All experiments were approved by the Florey Institute of Neuroscience and Mental Health Animal Ethics Committee (18-055-FINMH) and performed in accordance with the NHMRC Code of Practice for the Use of Animals for Scientific Purposes.

### 2.2. *In situ* perfused brainstem preparation

Experiments were performed using the *in situ* working-heart brainstem preparation (WHBP) of rats. Basic procedures were performed in

accordance with previously published studies (Dutschmann et al., 2000; Paton, 1996). In short, rats were deeply anaesthetized via inhalation of isoflurane (Zoetis, Sydney, Australia) until complete loss of the hindpaw withdrawal reflex in response to noxious pinch. They were bisected below the diaphragm, and immediately immersed in ice-cold Ringer's solution, skinned and decerebrated at the pre-collicular level. The cerebellum was removed for optimum visualization of the dorsal brainstem surface. The preparation was eviscerated, leaving the heart intact. The right thoracic phrenic nerve, the left recurrent laryngeal nerve and the left thoracic sympathetic chain (at the level of T10) were isolated and cut distally to record their efferent activities. The descending aorta was cannulated and perfused retrogradely with carbogenated Ringer's solution heated to 31 °C using a peristaltic pump (Watson & Marlow 505 S, Falmouth, UK) in order to maintain the eupneic three-phase respiratory motor pattern with constant respiratory drive, which was obtained at flow rates of 18–22 ml/min, which yielded perfusion pressures between 40 and 70 mmHg.

The perfusate was an isosmotic Ringer's solution (containing, in mM: NaCl, 125.00; NaHCO<sub>3</sub>, 24.00; KCl, 3.00; CaCl<sub>2</sub>, 2.50; MgSO<sub>4</sub>, 1.25; KH<sub>2</sub>PO<sub>4</sub>, 1.25; and glucose, 10.00) containing an oncotic agent (0.45% sucrose), bubbled with carbogen (95% O<sub>2</sub> and 5% CO<sub>2</sub>), pH 7.4 after carbogenation, and filtered using a nylon screen (pore size 100 µm; Millipore, Tullagreen, Ireland). After respiratory-related movements commenced, a neuromuscular blocker (vecuronium bromide, 300 µg/200 ml perfusate, Mylan, Brisbane, Australia) was added to the perfusate. The eupneic respiratory pattern was obtained by stimulating the peripheral chemoreflex with a bolus injection of NaCN (100 µL, 0.1% w/v).

### 2.3. Nerve recordings

Activities of the phrenic (PNA) and the thoracic sympathetic nerve (t-SNA) were recorded from cut proximal nerve ends using suction electrodes. The vagal postinspiratory motor pattern was recorded from the recurrent laryngeal nerve (RLNA) in order to preserve the connectivity between CVMs and the heart. An additional electrode was used to record the ECG to measure heart rate (HR). Signals were amplified (differential amplifier DP-311, Warner instruments, Hamden, USA), band-pass filtered from 100 Hz to 10 kHz, digitized (PowerLab/16SP ADInstruments, Sydney Australia) and then viewed and recorded using LabChart (version 7.0, ADInstruments).

### 2.4. Experimental protocols

Seven experimental groups were used to investigate the role of glycinergic inhibition in respiratory pattern formation and, consequently, the respiratory modulation in the RSA of the heart. In the first experimental group, the glycine receptor antagonist strychnine was added systemically to the perfusate (n = 7). After the preparation stabilized and developed the characteristic three-phase respiratory pattern and expressed a consistent RSA, a minimum of 10 min baseline period was recorded. Then, a dose-response curve for systemic strychnine application was measured by gradually increasing the systemic concentration to 50, 100 and 200 nM with a 10 min interval between strychnine administrations. In addition, to control the potential time-dependent changes of the eupneic three-phase respiratory pattern, the pattern of thoracic sympathetic nerve discharge or the strength of the RSA, we performed a series of time control experiments (n = 7). Representative recordings of the time control illustrate that all recorded cardio-respiratory or sympathetic-respiratory parameters remained unchanged throughout the duration of the experimental protocols (Suppl. Fig. 1). In the remaining five experimental groups, we measured the effects of local glycine receptor antagonism in each of five brainstem nuclei of the cardio-respiratory pattern generating network.

Local bilateral microinjections of strychnine were performed using triple-barrel borosilicate glass micropipettes, that also included a barrel containing 10 mM L-glutamate used to functionally identify the target

sites and a barrel containing Chicago sky blue dye (2% w/v) for *post-hoc* histological verification of the microinjection sites. The volume was controlled by viewing the movement of the meniscus through a binocular microscope fitted with an eyepiece reticule.

Once the cardio-respiratory motor pattern of each preparation stabilized, the pre-BötC ( $n = 6$ ), BötC ( $n = 7$ ), NTS ( $n = 7$ ), KFn ( $n = 7$ ) or NA/CVLM ( $n = 6$ ) were initially functionally characterized by unilaterally injecting glutamate (50 nl, 10 mM), which evoked a brief bradypneic response in BötC, NTS, KFn or NA/CVLM, whereas in preBötC, a short tachypnea was observed. In addition, glutamate microinjection in the NA/CVLM also evoked a brief bradycardia. Following the initial functional identification of the target site, bolus microinjections of strychnine (40–50 nl, 300  $\mu$ M) were performed via a multi-barreled micropipette. In preliminary experiments with strychnine microinjection into the pre-BötC at concentrations of 50 and 200  $\mu$ M, we did not observe any significant response, whereas a 300  $\mu$ M concentration induced distinctive physiological responses. Therefore, this minimal 300  $\mu$ M concentration of strychnine (diluted in Ringer's solution) was used for all strychnine microinjections to avoid off-target effects of strychnine at high concentrations. Finally, Chicago sky blue dye was microinjected to label the injection sites. This procedure was then repeated on the contralateral side. The respiratory parameters and RSA were monitored for at least 10 min after the bilateral microinjections.

The injections into the pre-BötC were performed at 1.4–1.5 mm rostral to *calamus scriptorius*, 1.9 mm lateral to midline and 2.0 mm ventral to the dorsal surface of medulla, whilst the injections into the BötC followed the same lateral and dorsal-ventral coordinates, but 1.7–1.9 mm rostral to *calamus scriptorius*. For the pontine KFn, the coordinates were 0.2–0.5 mm caudal to the caudal end of inferior colliculus, 2.0–2.5 mm lateral to midline and 1.0–1.2 mm ventral to the dorsal surface. At the NTS, the bilateral injections were performed in two different sites in order to cover the entire extent of intermediate and caudal NTS. The coordinates for the first injection were 0.2–0.3 mm rostral to *calamus scriptorius* and 0.3–0.4 mm lateral to midline, whilst the second spot was at 0.2 mm caudal to *calamus scriptorius* and 0.2 mm lateral to midline. For both injections, the depth was 0.4 mm ventral to the dorsal surface of the medulla. Finally, we targeted the CVLMs in caudal NA with the following coordinates: 0.0–0.1 mm rostral to *calamus scriptorius*, 1.7–1.9 mm lateral to midline and 1.8–2.0 mm ventral to the dorsal surface. The NA has a small surface area and it is inevitable that 60 nl strychnine microinjections will spread into the adjacent CVLM, therefore we term these injection sites NA/CVLM throughout the remainder of the manuscript.

At the end of the experiments, the perfusion was stopped in order to measure the electrical DC-noise level in t-SNA to subtract this offset in further analysis.

### 2.5. Histological analyses of microinjection sites

At the end of the microinjection experiments, the brainstems were removed and post-fixed in 4% paraformaldehyde for 3–5 days before being transferred to 0.1 M phosphate buffered saline containing 20% sucrose for 2 days. A cryostat (Leica Biosystems) was used to section the brainstem (40  $\mu$ m thickness). Sections were mounted and counterstained with 1% Neutral Red (Sigma-Aldrich) to validate anatomical location of injection sites. The locations of microinjections are documented in schematic drawings of coronal sections (Fig. 7) and photographs (suppl. Fig. 2).

### 2.6. Data analysis

Analysis of cardio-respiratory motor activities were performed in Spike2 (Version 7.17, Cambridge Electronic Design, Cambridge, UK). All analyses were performed in intervals containing 20 consecutive respiratory cycles. For the assessment of systemic effects of strychnine on cardio-respiratory patterning, the analyses were performed immediately

before the application of the first dose of strychnine (baseline interval) and 5 min after each additional application of strychnine (50, 100 and 200 nM) into the perfusate. To evaluate the changes in cardio-respiratory patterning evoked by strychnine microinjection, the analyses were performed in period immediately prior to the glutamate injection (baseline interval) and at 1, 5 and 10 min following the completion of the bilateral strychnine microinjection. For the time-control group, a baseline interval was analyzed following the stabilization of the preparation. Since it was needed an average of 5 min to complete the bilateral microinjections in the experimental groups, for the control group the analyses were performed at 6, 10 and 15 min after the baseline interval.

PNA, RLNA and t-SNA were first rectified and integrated (50 ms time constant). The respiratory frequency ( $F_R$ ), duration of inspiration ( $T_I$ ) and total respiratory cycle length ( $T_{TOT}$ ) were determined from the onset and offset times of inspiration (inspiratory on-switch and off-switch) as reflected in the integrated PNA time series. The duration of the post-inspiratory ( $T_{PI}$ ) and late-expiratory ( $T_{E2}$ ) phases were measured from integrated RLNA. The  $T_{PI}$  was calculated considering the time interval from the inspiratory off-switch to the time when integrated RLNA reached zero (e.g., the start of late-expiration).  $T_{E2}$  was the interval in which the RLNA remained silent until the inspiratory on-switch of the next respiratory cycle. Finally, we quantified the time between the inspiratory off-switch and the onset of the RLNA-peak discharge (IOS to PI peak) to detect potential a shift of postinspiratory discharge into the inspiratory phase of respiratory motor cycle (e.g. [Dutschmann and Paton, 2002a](#)).

Heart rate (HR) was measured from the R-R interval between consecutive ECG events. The magnitude of the RSA was quantified as the peak-to-trough difference in HR within each respiratory cycle. These HR changes were measured relative to the inspiratory off-switch (PNA burst termination) to specifically quantify the inspiratory-related tachycardia and the postinspiratory bradycardia of the RSA. The mean baseline heart rate of the RSA measures was determined from the time point of cessation of RLNA postinspiratory discharge (mid to late expiration) when HR has a transient steady state. In addition, cycle-triggered averages of the RSA and t-SNA were triggered from the inspiratory off-switch and used to qualitatively analyze their patterns of cardio-respiratory coupling. The instantaneous values of RSA, RLNA, PNA and t-SNA in each fraction of the respiratory cycle were normalized to their mean values within the interval analyzed.

Statistical tests were performed with one-way repeated measure ANOVA followed by Student-Newman-Keuls *post hoc* test (SigmaPlot version 11.0). P-values less than 0.05 were considered statistically significant. All values are expressed as mean  $\pm$  SEM.

## 3. Results

At baseline, recordings of PNA, RLNA, HR and t-SNA displayed their characteristic cardio-respiratory patterns in all groups (See Fig. 1-6Ai, Bi): (i) an eupneic, three-phase respiratory motor pattern of ramping inspiratory PNA, biphasic inspiratory (I) and postinspiratory (PI) RLNA with the peak discharge occurring at the I-PI phase transition, (ii) a robust RSA characterized by inspiratory-related tachycardia and postinspiratory-related bradycardia, and (iii) an inspiratory bursting of t-SNA.

### 3.1. Effects of systemic GlyR blockade on cardio-respiratory coupling

The effects of systemic application of 50 nM strychnine are illustrated by original recordings and cycle trigger averages in Fig. 1Aii & 1Bii. Systemic blockade of GlyRs ( $n = 7$  preparations) at a concentration of 50 nM strychnine significantly decreased the magnitude of the RSA without any change in sympatho-respiratory coupling (Fig. 1Bii). In addition, 50 nM strychnine evoked a significant increase in  $F_R$  and a significant decrease in the  $T_I$ ,  $T_{PI}$  and  $T_{TOT}$  (Table 1). However, the eupneic three-phase respiratory motor pattern (inspiration, post-inspiration and late-

**Table 1**  
Summary of strychnine evoked changes in respiratory parameters.

Injection site	FR(bpm)		TI(s)		TPI(s)		TE2(s)		TTOT(s)	
	baseline	strychnine	baseline	Strychnine	baseline	strychnine	baseline	strychnine	baseline	strychnine
NA/CVLM	17.6 ± 0.9	24.9 ± 2.4**	0.8 ± 0.1	0.5 ± 0.0***	2.0 ± 0.1	1.3 ± 0.1	0.8 ± 0.2	0.9 ± 0.3	3.5 ± 0.2	2.7 ± 0.3**
NTS	14.0 ± 1.9	17.1 ± 2.2**	0.9 ± 0.1	0.8 ± 0.1*	3.0 ± 0.5	1.7 ± 0.4**	0.8 ± 0.2	1.3 ± 0.2	4.8 ± 0.5	3.8 ± 0.4**
pre-BötC	14.5 ± 0.9	15.8 ± 1.4	1.0 ± 0.1	0.8 ± 0.1*	2.4 ± 0.3	2.3 ± 0.3	0.9 ± 0.1	0.8 ± 0.1	4.2 ± 0.2	4.0 ± 0.3
BötC	14.9 ± 1.8	15.1 ± 2.0	0.9 ± 0.1	0.7 ± 0.0**	2.7 ± 0.4	2.8 ± 0.7	1.3 ± 0.3	1.1 ± 0.1	4.9 ± 0.7	4.6 ± 0.7
KFn	12.0 ± 0.9	13.7 ± 1.1*	1.0 ± 0.1	0.9 ± 0.1	3.3 ± 0.4	2.6 ± 0.3*	1.1 ± 0.3	1.0 ± 0.2	5.4 ± 0.4	4.5 ± 0.4*
systemic (50 nM)	14.1 ± 1.1	18.5 ± 1.5**	1.0 ± 0.1	0.8 ± 0.0*	2.6 ± 0.3	1.7 ± 0.3***	0.8 ± 0.2	1.0 ± 0.3	4.5 ± 0.3	3.5 ± 0.3***
systemic (100 nM)	14.1 ± 1.1	22.8 ± 1.6***	1.0 ± 0.1	0.6 ± 0.1**	2.6 ± 0.3	1.5 ± 0.3***	0.8 ± 0.2	0.8 ± 0.2	4.5 ± 0.3	2.9 ± 0.2***
systemic (200 nM)	14.1 ± 1.1	24.7 ± 2.1***	1.0 ± 0.1	0.7 ± 0.1*	2.6 ± 0.3	1.4 ± 0.3***	0.8 ± 0.2	0.6 ± 0.1	4.5 ± 0.3	2.6 ± 0.3***
control (10 min)	15.6 ± 1.1	16.2 ± 1.4	0.8 ± 0.1	0.8 ± 0.1	2.1 ± 0.3	2.1 ± 0.3	1.2 ± 0.2	1.1 ± 0.1	4.0 ± 0.3	3.9 ± 0.4

Abbreviations: FR = respiratory frequency; TI = inspiratory phase duration; TPI = postinspiratory phase duration; TE2 = expiratory (stage 2) phase duration. BötC = Bötzinger complex, KFn = Kölliker-Fuse nuclei, NA/CVLM, Nucleus ambiguus/caudal ventrolateral medulla, NTS = nucleus of the solitary tract; pre-BötC = pre-Bötzinger complex.

expiration) was preserved. Increasing the systemic strychnine concentration to 100 nM triggered a further decrease in the magnitude of RSA without a change in the respiratory-coupled t-SNA pattern (Fig. 1Aiii, Biii). Administration of 100 nM strychnine further increased  $F_R$  via reductions in  $T_I$ ,  $T_{PI}$  (Table 1). At the final strychnine concentration of 200 nM, the RSA was abolished. Further, the RLNA peak discharge was shifted significantly from postinspiration at baseline to late-inspiration after systemic strychnine administration (Fig. 1D) consistent with previous reports (Dutschmann & Paton, 2002a, 2002b, 2002c). At 200 nM strychnine the t-SNA burst was shifted from inspiration to postinspiration (Fig. 1Biii). However, this effect has only been observed after highest doses of systemic strychnine and is not further discussed.

### 3.2. Effects of local GlyR blockade in the nucleus ambiguus/caudal ventrolateral medulla (NA/CVLM)

To study the effects of GlyR antagonism at level of the CVLMs, we microinjected strychnine (300  $\mu$ M) into the NA/CVLM region ( $n = 6$ , see Fig. 7A and suppl Fig. 2). Five minutes after bilateral strychnine injections, a clear effect on the expression of RSA in original recordings was observed (Fig. 2A). The cycle-triggered averages in Fig. 2Bii illustrate the significant reduction in the inspiratory tachycardia of the RSA ( $+9 \pm 3$  bpm vs. baseline  $+34 \pm 13$  bpm,  $p < 0.05$ ; Fig. 2C) and postinspiratory bradycardia of the RSA ( $-8 \pm 7$  bpm vs. baseline  $-27 \pm 9$  bpm,  $p < 0.05$ ; Fig. 2C). In addition to the effect on RSA, blockade of GlyRs in the NA/CVLM triggered a significant change in the baseline respiratory rhythm (Fig. 2A and B) that was characterized by a 41% increase in  $F_R$  ( $p < 0.001$ ; Table 1) ( $+41 \pm 12\%$ ,  $p < 0.001$ ; Table 1), a shortening in  $T_I$  by 32% ( $p < 0.001$ ; Table 1) and a decrease in  $T_{TOT}$  by 24% ( $p < 0.01$ ; Table 1). The cycle-triggered averages of PNA and RLNA showed that the strychnine injection into the NA/CVLM region triggered a shift in the peak discharge of RLNA from post-inspiration to inspiration (Fig. 2A and B) as observed after systemic application of 200 nM strychnine (see Fig. 1Aiv, D). The observed change in the RLNA discharge pattern was comparable to effect observed previously (e.g. Dutschmann and Paton, 2002a) and thus indicates a shift of postinspiratory activity into the inspiratory phase determined by the simultaneously recorded PNA. Finally, systemic GlyR blockade, strychnine microinjections in the NA/CVLM did not change the magnitude or timing of respiratory-related t-SNA bursts (Fig. 2A and B).

### 3.3. Effects of local GlyR blockade in the nucleus of the solitary tract (NTS)

Five minutes after the bilateral strychnine microinjection in the NTS ( $n = 7$ ; see Fig. 7B and suppl Fig. 2), a substantial decrease in the magnitude of the RSA was observed (Fig. 3A and B). This effect was due to a significant decrease in the inspiratory-related tachycardia ( $+5 \pm 1$  bpm vs. baseline  $+13 \pm 4$  bpm,  $p < 0.05$ ; Fig. 3C). The postinspiratory bradycardia, however, was not significantly changed ( $-11 \pm 4$  bpm vs.

baseline  $-8 \pm 2$  bpm; Fig. 3C). GlyR blockade in the NTS did not evoke any change in the eupneic three-phase respiratory motor pattern in PNA or RLNA (Fig. 3). It was observed an increase in  $F_R$  by 24% ( $p < 0.01$ ; Table 1) and significant decreases in  $T_{PI}$  by 42% ( $p < 0.01$ ; Table 1),  $T_I$  by 10% ( $p < 0.05$ ; Table 1) and  $T_{TOT}$  by 19% ( $p < 0.01$ ; Table 1). Finally, GlyR blockade in the NTS had no effect on sympatho-respiratory coupling as seen in t-SNA (Fig. 3A and B).

### 3.4. Effects of local inhibition of GlyR in the pre-Bötzinger complex (pre-BötC)

We next evaluated the involvement of GlyR in the pre-BötC ( $n = 6$ ; see Fig. 7C and suppl Fig. 2) on the generation of the respiratory motor pattern and cardio-respiratory coupling. Bilateral strychnine microinjection in the pre-BötC evoked a modest decrease in the magnitude of RSA (Fig. 4A–C). The decrease in the RSA was mediated by a significant decrease in the inspiratory-related tachycardia ( $+15 \pm 3$  bpm vs. baseline  $+28 \pm 7$  bpm,  $p < 0.05$ ; Fig. 4C), while postinspiratory bradycardia remained unchanged ( $-21 \pm 4$  bpm vs. baseline  $-20 \pm 5$  bpm; Fig. 4C). Local GlyR blockade in the pre-BötC did not evoke changes in either the PNA or RLNA discharge patterns (Fig. 4A and B) or the timing of the postinspiratory RLNA burst (Fig. 4D). Also, GlyR blockade in the pre-BötC had little effects on other respiratory parameters (Table 1) except a small but significant decrease in  $T_I$  by 15% ( $p < 0.05$ ; Table 1). Sympatho-respiratory coupling reflected in t-SNA was also not affected by GlyR blockade in the pre-BötC (Fig. 4A and B).

### 3.5. Effects of local inhibition of GlyR in the Bötzinger complex (BötC)

Bilateral injections of strychnine in the BötC ( $n = 7$ ; see Fig. 7D and suppl Fig. 2) did not evoke any relevant change in the expression of RSA (Fig. 5C) and also did not evoke any significant changes in the respiratory motor pattern, respiratory parameters or sympatho-respiratory coupling (Fig. 5, Table 1).

### 3.6. Effects of local inhibition of GlyR in the Kölliker-Fuse nuclei (KFn)

The pontine KFn was identified as a brainstem area critical for the generation of RSA (Farmer et al., 2016). GlyR blockade in the KFn triggered a significant decrease in the magnitude of the RSA as illustrated in representative traces and cycle triggered averages (Fig. 6A and B). The change in RSA following strychnine microinjections into the KFn ( $n = 7$ ; see Fig. 7E and suppl Fig. 2) was due to a significant decrease in the inspiratory-related tachycardia ( $+11 \pm 2$  bpm vs. baseline  $+21 \pm 4$  bpm,  $p < 0.05$ ; Fig. 6C). However, the postinspiratory bradycardia was not significantly changed ( $-8 \pm 3$  bpm vs. baseline  $-11 \pm 4$  bpm; Fig. 6C). GlyR blockade in the KFn did not change the three-phase respiratory motor pattern expressed in PNA and RLNA (Fig. 6B) or the timing of the RLNA-peak discharge in relation to PNA burst termination (Fig. 6D).

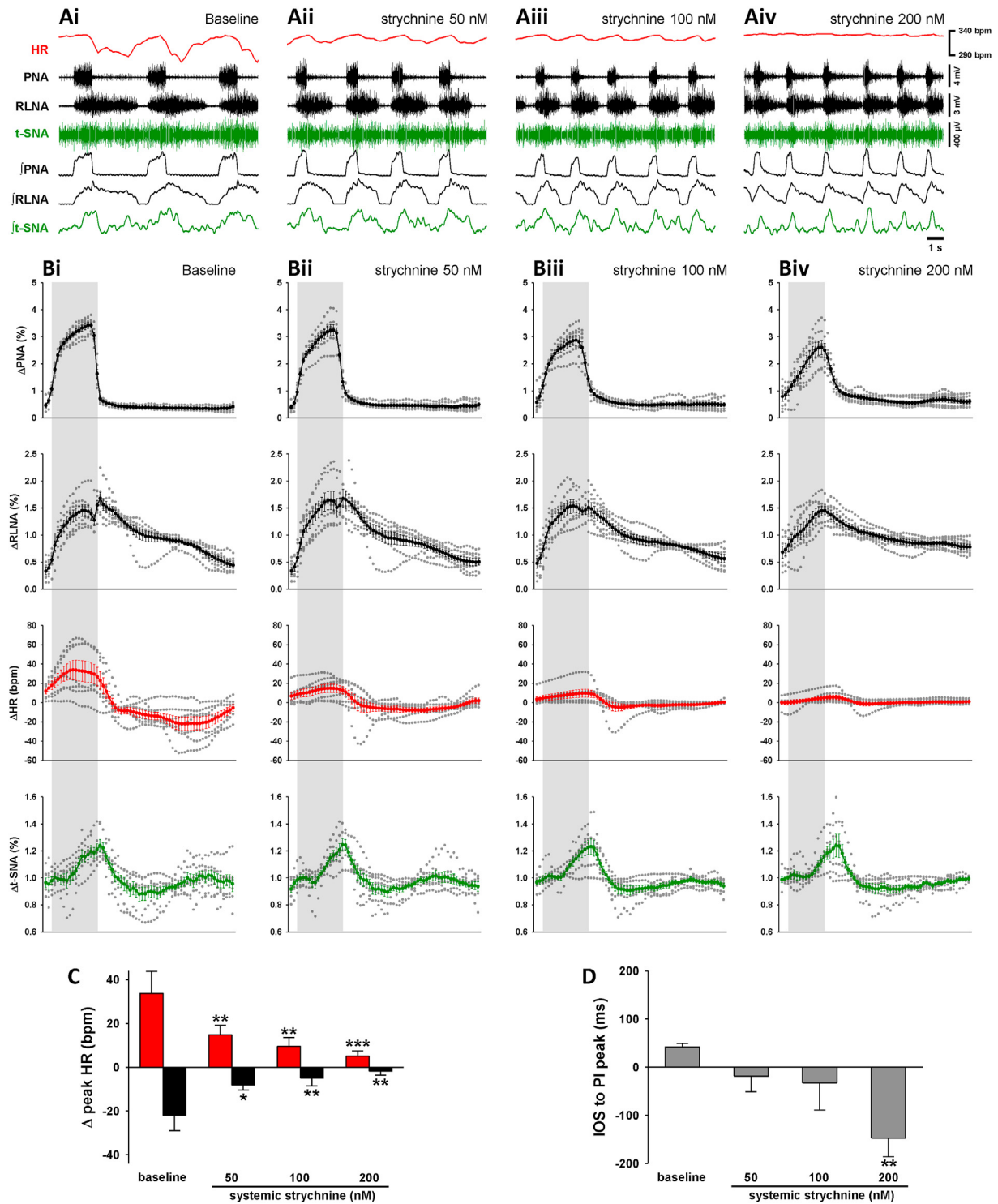


**Fig. 1. Systemic strychnine abolishes the RSA.** Raw and integrated ( $\int$ ) representative recordings of phrenic (PNA), recurrent laryngeal nerve (RLNA) and thoracic sympathetic nerve (t-SNA) activities and heart rate (HR, red tracings) at baseline (Ai) and after systemic application of strychnine 50 nM (Aii), 100 nM (Aiii) and 200 nM (Aiv). Normalized (no time axis) cycle-triggered averages of PNA, RLNA, HR and t-SNA obtained at baseline (Bi) and after systemic strychnine 50 nM (Bii), 100 nM (Biii) and 200 nM (Biv). The thick lines indicate the average activity of 7 *in situ* preparations, whereas the dotted lines indicate the individual values of each preparation. The shaded grey areas indicate the inspiratory phase. Note the blunting in RSA and the change in the respiratory pattern induced by the glycinergic antagonist. The magnitude of the RSA ( $\Delta$  peak HR) was split in inspiratory tachycardia (red bars) and post-inspiratory bradycardia (black bars) (C). Both inspiratory tachycardia and post-inspiratory bradycardia decrease progressively with increasing doses of strychnine. The time interval between the inspiratory off-switch (IOS) and the RLN post-inspiratory peak also decreases with strychnine (D). The post-inspiratory peak shifts to late inspiration with strychnine 200 nM. Data are presented as mean  $\pm$  SEM; n = 7 preparations; \* $p < 0.05$  vs. baseline; \*\* $p < 0.01$  vs. baseline; \*\*\* $p < 0.001$  vs. baseline.

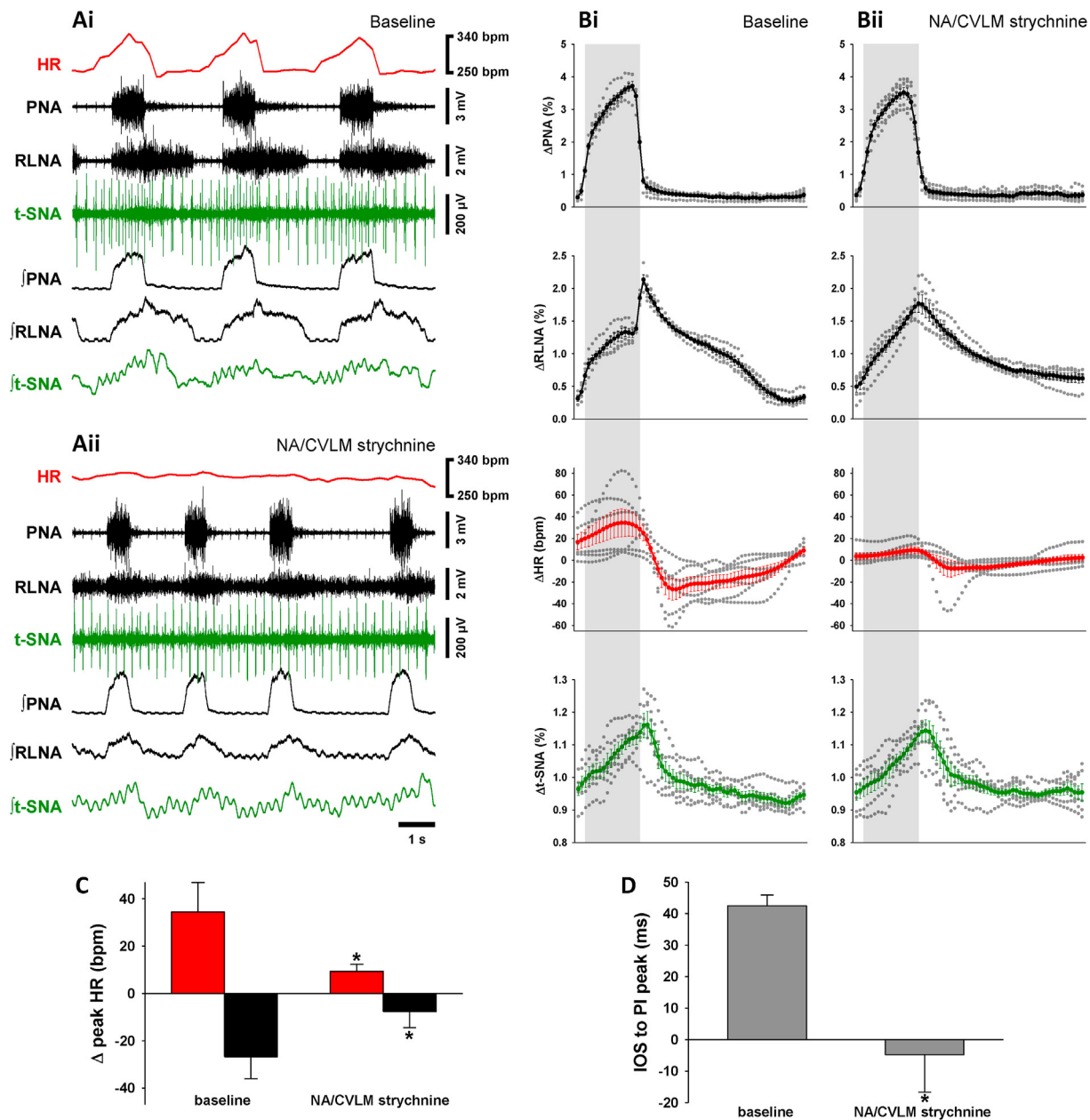


**Fig. 2. Strychnine in the NA/CVLM inhibits the RSA.** Raw and integrated (*f*) representative recordings of phrenic (PNA), recurrent laryngeal nerve (RLNA) and thoracic sympathetic nerve (t-SNA) activities and heart rate (HR, red tracings) during baseline (Ai) and 5 min after bilateral microinjection of strychnine in the NA/CVLM (Aii). Normalized (no time axis) cycle-triggered averages of PNA, RLNA, HR and t-SNA obtained at baseline (Bi) and 5 min following the strychnine injection in the NA/CVLM (Bii). The thick lines indicate the average activity of 6 *in situ* preparations, whereas the dotted lines indicate the individual values of each preparation. The shaded grey areas indicate the inspiratory phase. Note the glycinergic antagonist almost abolishes the RSA. The magnitude of the RSA ( $\Delta$  peak HR) was split in inspiratory tachycardia (red bars) and post-inspiratory bradycardia (black bars) (C). Both inspiratory tachycardia and post-inspiratory bradycardia decrease 5 min after the strychnine. The glycinergic antagonist in the NA/CVLM also induced a shift of the peak of the RLN from post-inspiration to late inspiration (D). Data are presented as mean  $\pm$  SEM; *n* = 7 preparations; \**p* < 0.05 vs. baseline.

GlyR blockade in the KFn induced a significant increase in  $F_R$  by 15% (*p* < 0.05, Table 1) and a decrease of  $T_{PI}$  by 20% (*p* < 0.05, Table 1) and  $T_{TOT}$  by 16% (*p* < 0.05, Table 1).

#### 4. Discussion

Systemic application of strychnine triggered significant effects on cardio-respiratory activity patterns. Blocking glycinergic neurotransmission largely abolished the respiratory sinus arrhythmia (RSA). In parallel, a shift of the postinspiratory peak discharge of the recurrent laryngeal nerve into inspiration was observed. Strychnine

microinjections targeting the nucleus ambiguus and surrounding caudal ventrolateral medulla oblongata (NA/CVLM) resembled the above described effects of systemic glycine receptor GlyR blockade. However, at level of the primary respiratory pattern generating pre-motoneuron populations of the ponto-medullary respiratory network, local GlyR blockade triggered subtle modulation of respiratory rate or changes in respiratory phase duration, but had remarkably little effect on the timing a sequential timing of postinspiratory motor bursting. Contrary, strychnine injected into the same pontomedullary pre-motor populations produced a consistent and fairly uniform attenuation of the inspiratory RSA tachycardia (for details see below).

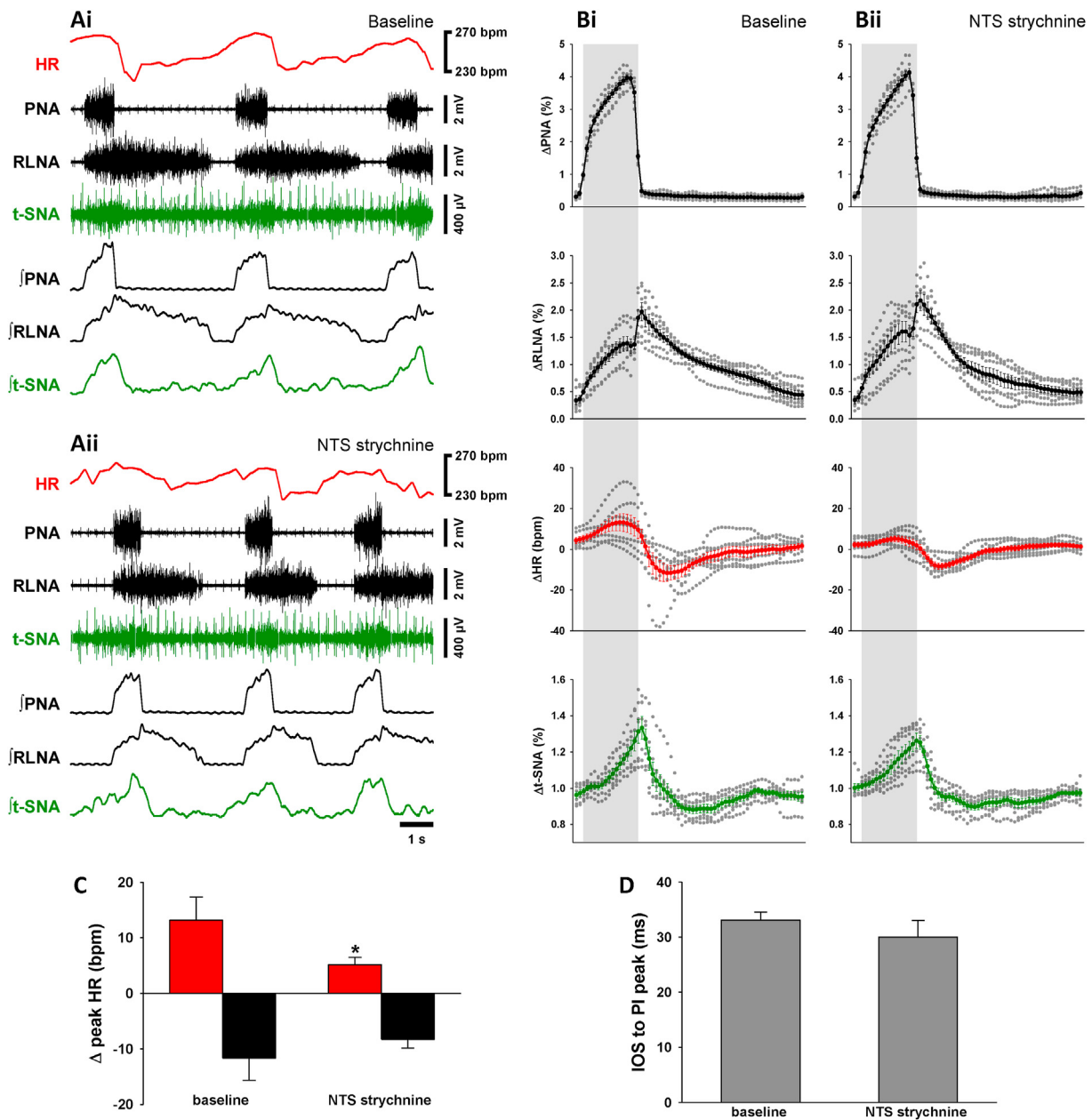


**Fig. 3. Strychnine in the NTS inhibits the RSA.** Raw and integrated (*f*) representative recordings of phrenic (PNA), recurrent laryngeal nerve (RLNA) and thoracic sympathetic nerve (t-SNA) activities and heart rate (HR, red tracings) during baseline (Ai) and 5 min after bilateral microinjection of strychnine in the NTS (Aii). Normalized (no time axis) cycle-triggered averages of PNA, RLNA, HR and t-SNA obtained at baseline (Bi) and 5 min following the strychnine injection in the NTS (Bii). The thick lines indicate the average activity of 7 *in situ* preparations, whereas the dotted lines indicate the individual values of each preparation. The shaded grey areas indicate the inspiratory phase. Note the glycinergic antagonist decreases the respiratory fluctuation of the HR. The magnitude of the RSA ( $\Delta$  peak HR) was split in inspiratory tachycardia (red bars) and post-inspiratory bradycardia (black bars) (C). The inspiratory tachycardia decreases whereas the post-inspiratory bradycardia did not change 5 min after the strychnine in the NTS. The time interval between the inspiratory off-switch (IOS) and the RLN post-inspiratory (PI) peak did not change after strychnine (D). Data are presented as mean  $\pm$  SEM; n = 7 preparations; \**p* < 0.05 vs. baseline.

In summary, the present study identified that: (i) inhibitory glycinergic pre-motor drive during the inspiratory phase shapes the activity patterns of cardiac vagal motoneurons (CVMs) and consequently RSA, and (ii) glycinergic inhibition is involved in the local modulation of respiratory frequency and phase duration and specifically controls the inspiratory inhibition of postinspiratory laryngeal motoneurons (LMNs).

#### 4.1. Central origins of cardio-respiratory coupling

Cardio-respiratory coupling, which underpins the integrative function of autonomic brainstem circuits to control vital mechanisms of

oxygen uptake, pulmonary gas exchange and oxygen transport, is a major research focus in the field of neurophysiology (Anrep et al., 1936; Ben-Tal et al., 2012; Dick et al., 2009, 2014; Hayano et al., 1996). Previous research studies accumulate into the working hypothesis that the oscillation in CVM activity between inhibition during inspiration (Gilbey et al., 1984; Iriuchijima and Kumada, 1964; Kunze, 1972; McAllen and Spyer, 1978) and excitation and/or disinhibition during postinspiration (Farmer et al., 2016) are mechanisms that generate the RSA.

The present study aimed to identify sources of inspiratory CVM inhibition such as the NTS, pre-BötC and KFn. Our investigations did not identify a single source of CVM inhibition, but instead, local GlyR

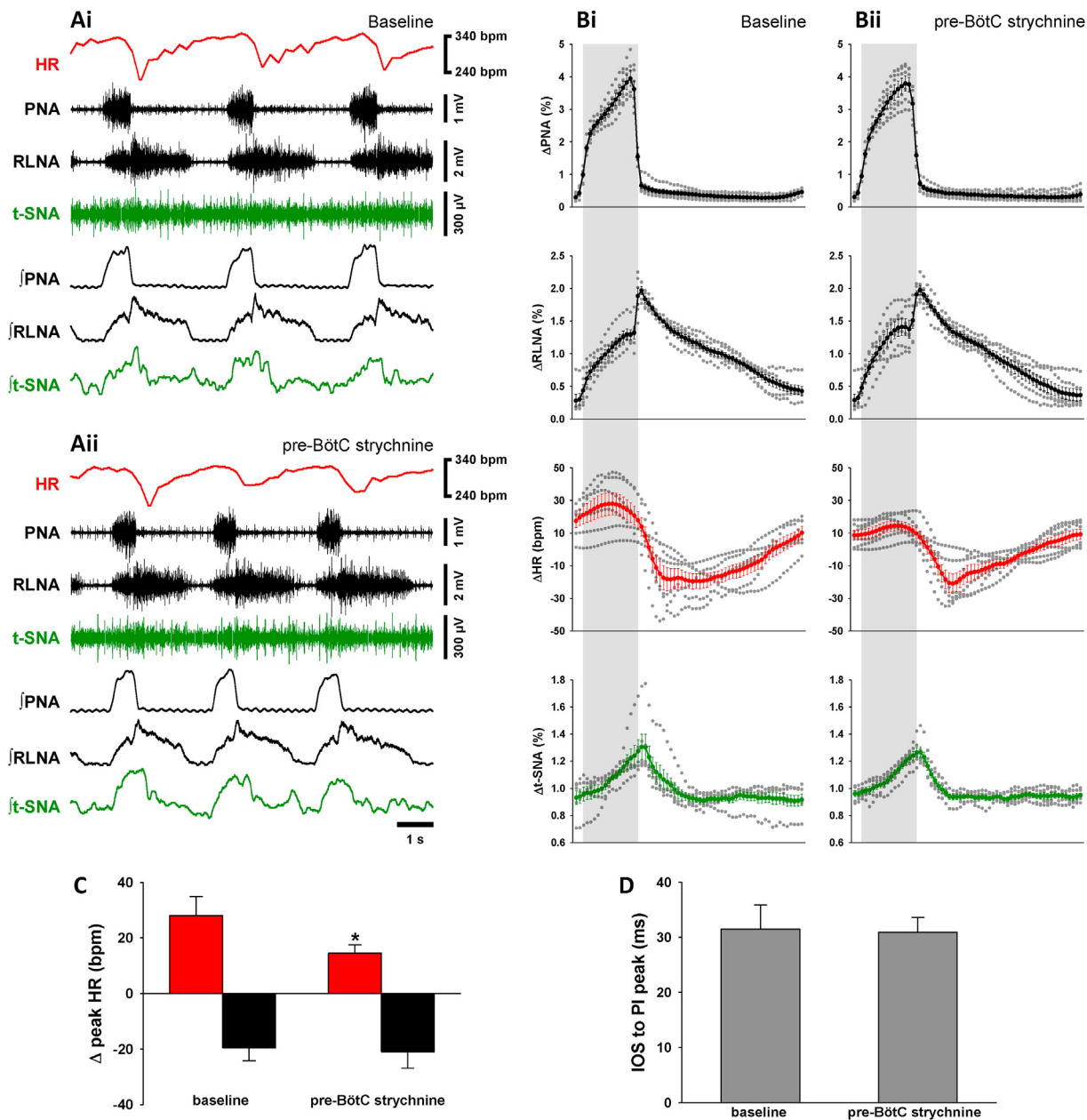


**Fig. 4. Strychnine in the pre-BötC inhibits the RSA.** Raw and integrated ( $\int$ ) representative recordings of phrenic (PNA), recurrent laryngeal nerve (RLNA) and thoracic sympathetic nerve (t-SNA) activities and heart rate (HR, red tracings) during baseline (Ai) and 5 min after bilateral microinjection of strychnine in the pre-BötC (Aii). Normalized (no time axis) cycle-triggered averages of PNA, RLNA, HR and t-SNA obtained at baseline (Bi) and 5 min following the strychnine injection in the pre-BötC (Bii). The thick lines indicate the average activity of 6 *in situ* preparations, whereas the dotted lines indicate the individual values of each preparation. The shaded grey areas indicate the inspiratory phase. Note the glycinergic antagonist slightly diminishes the RSA. The magnitude of the RSA ( $\Delta$  peak HR) was split in inspiratory tachycardia (red bars) and post-inspiratory bradycardia (black bars) (C). The inspiratory tachycardia decreases whereas the post-inspiratory bradycardia remained unchanged 5 min after the strychnine in the pre-BötC. The time interval between the inspiratory off-switch (IOS) and the RLN post-inspiratory (PI) peak did not change after strychnine (D). Data are presented as mean  $\pm$  SEM; n = 6 preparations; \*p < 0.05 vs. baseline.

blockade in any of these nuclei uniformly produced a fairly selective attenuation of tachycardic component of the RSA. It is important to note that GlyR blockade may rather disturb the local balance of synaptic excitation and inhibition in the cardio-respiratory network, than it is functionally disrupting reciprocal synaptic inhibition of antagonistic cardio-respiratory neuron groups (see detailed discussion in 4.2). Thus, local perturbation of the inhibitory-excitatory balance identifies that inspiratory inhibition of CVMs is more likely determined by synaptic interactions within a distributed brainstem network, instead by a single source of input. Nevertheless, electrophysiological studies *in vitro* that lack the functional readout of heart rate suggested that GABAergic, and

to a lesser extent glycinergic inputs, to the CVMs during inspiration are the main source of CVM inhibition (Sharp et al., 2014). Since *in vitro* inspiratory activity in rhythmic slices is exclusively generated by the pre-Bötzing (pre-BötC) complex (Smith et al., 1991; Feldman and Del Negro, 2006), this brain circuit appears to be the designated source for a GABAergic/glycinergic inhibition of CVMs. Our data now confirm that glycinergic neurotransmission mediates CVM inhibition, since local blockade of GlyR was sufficient to ablate inspiratory tachycardia and consequently RSA at level of the NA. Moreover, systemic application or local strychnine microinjection into the NA/CVLM did not trigger significant changes in the baseline HR, suggesting that CVMs are not under

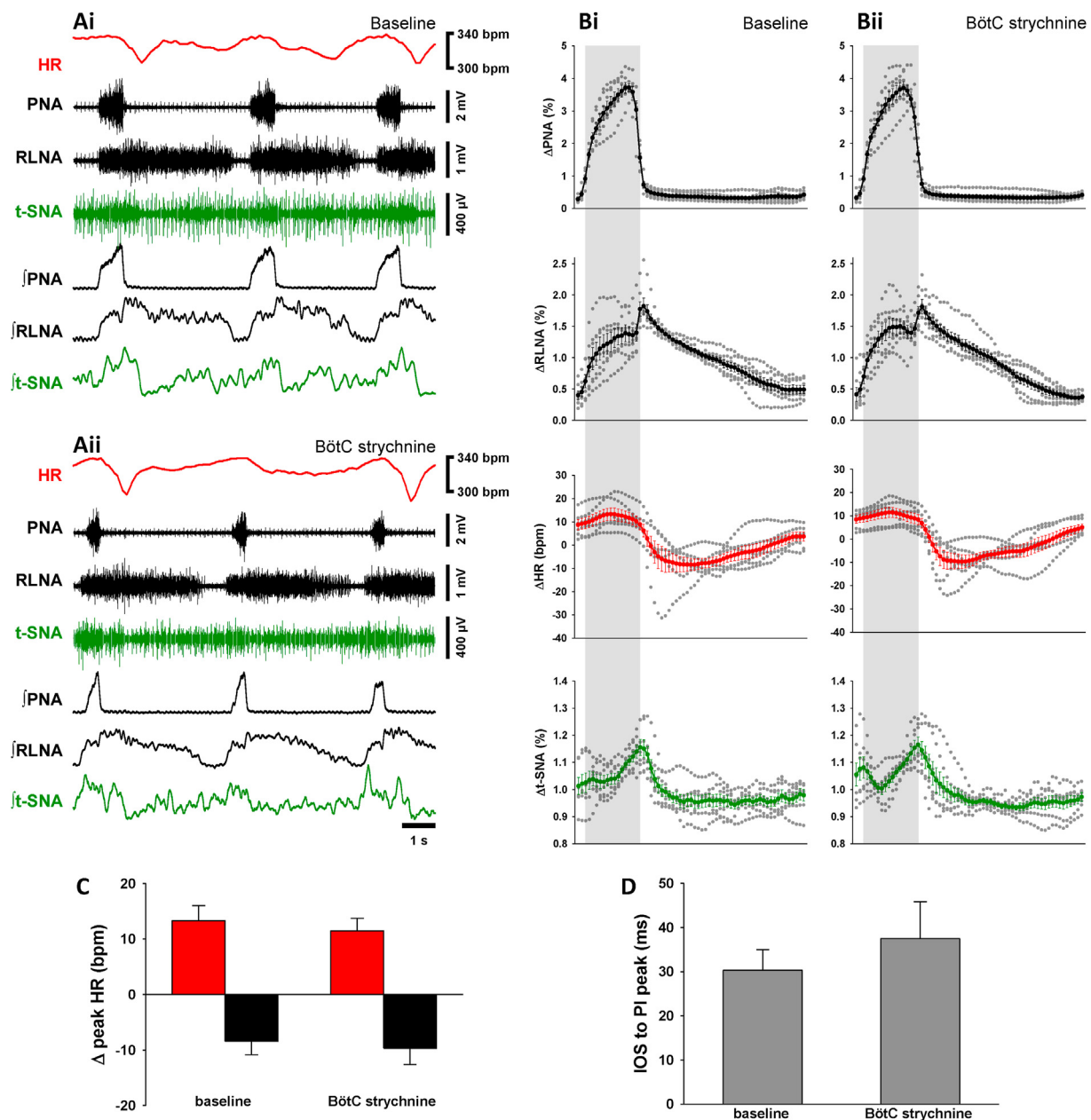


**Fig. 5. Strychnine in the BötC does not change the RSA.** Raw and integrated ( $\int$ ) representative recordings of phrenic (PNA), recurrent laryngeal nerve (RLNA) and thoracic sympathetic nerve (t-SNA) activities and heart rate (HR, red tracings) during baseline (Ai) and 5 min after bilateral microinjection of strychnine in the BötC (Aii). Normalized (no time axis) cycle-triggered averages of PNA, RLNA, HR and t-SNA obtained at baseline (Bi) and 5 min following the strychnine injection in the BötC (Bii). The thick lines indicate the average activity of 7 *in situ* preparations, whereas the dotted lines indicate the individual values of each preparation. The shaded grey areas indicate the inspiratory phase. Note the RSA remains unchanged 5 min after the strychnine. The magnitude of the RSA ( $\Delta$  peak HR) was split in inspiratory tachycardia (red bars) and post-inspiratory bradycardia (black bars) (C). Both inspiratory tachycardia and post-inspiratory bradycardia remain unchanged following strychnine microinjection in the BötC. The time interval between the inspiratory off-switch (IOS) and the RLN post-inspiratory (PI) peak also did not change with strychnine (D). Data are presented as mean  $\pm$  SEM; n = 7 preparations.

tonic glycinergic inhibition during intact network conditions. Thus, the data of the present study suggest that glycinergic inspiratory neurons modulate CVM activity. Inspiratory glycinergic neurons that could mediate such effect were indeed specifically identified in the pre-BötC (Winter et al., 2009; Morgado-Valle et al., 2010). Further support for this hypothesis is provided by a recent study that also suggested the pre-BötC as the source of CVM inhibition at intact network level (Menuet et al., 2020). Menuet and colleagues elegantly demonstrated that neurons in the pre-BötC project to CVMs and either the photoinhibition or photoexcitation of these neurons can modulate the magnitude of RSA. However, a major caveat of this study is that optogenetic manipulation of

pre-BötC neurons suppressed inspiration, but simultaneously activated postinspiratory network activity (also see Ausborn et al., 2018). Thus, optogenetic manipulation selectively modulated the bradycardic RSA component via downstream elements of the cardio-respiratory network. The potential sources of such downstream effects are most likely the pontine Kölliker-Fuse nuclei (KFn). Indeed previously it was demonstrated that RSA can be abolished after pharmacological inhibition of the KFn (Farmer et al., 2016) and after ponto-medullary brainstem transections (Baekey et al., 2008). However, the underlying mechanism that abolished RSA in these studies relates to the suppression of KFn mediated excitatory postinspiratory drive to CVMs that generates the bradycardic

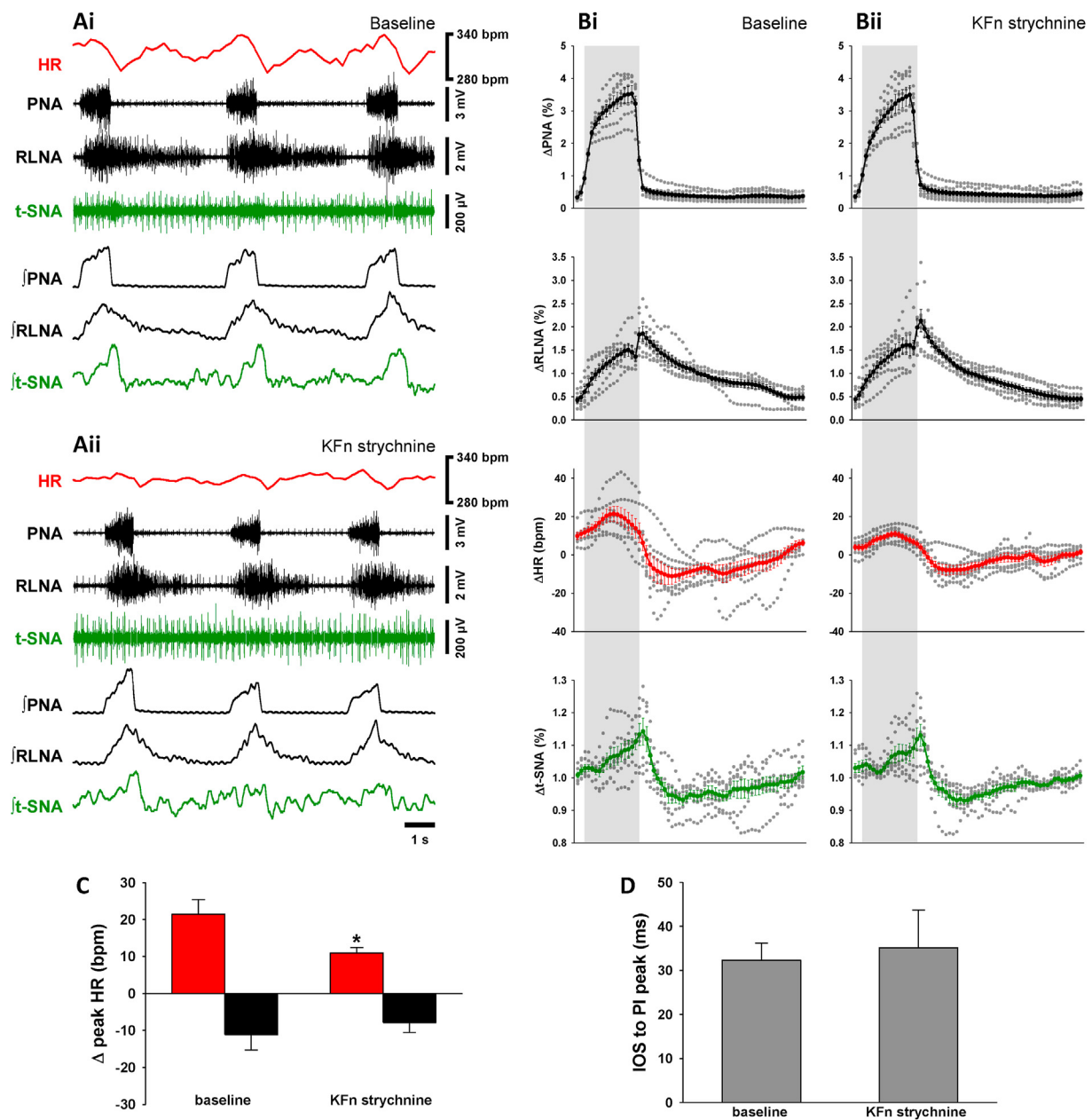


**Fig. 6. Strychnine in the KFn inhibits the RSA.** Raw and integrated ( $\int$ ) representative recordings of phrenic (PNA), recurrent laryngeal nerve (RLNA) and thoracic sympathetic nerve (t-SNA) activities and heart rate (HR, red tracings) during baseline (Ai) and 5 min after bilateral injection of strychnine in the KFn (Aii). Normalized (no time axis) cycle-triggered averages of PNA, RLNA, HR and t-SNA obtained at baseline (Bi) and 5 min following the strychnine microinjection in the KFn (Bii). The thick lines indicate the average activity of 7 *in situ* preparations, whereas the dotted lines indicate the individual values of each preparation. The shaded grey areas indicate the inspiratory phase. Note the strychnine injection in the KFn induced a decrease in the RSA. The magnitude of the RSA ( $\Delta$  peak HR) was split in inspiratory tachycardia (red bars) and post-inspiratory bradycardia (black bars) (C). While the post-inspiratory bradycardia remained unchanged, the inspiratory tachycardia decreases 5 min after the strychnine in the KFn. The time interval between the inspiratory off-switch (IOS) and the RLN post-inspiratory (PI) peak did not change after strychnine (D). Data are presented as mean  $\pm$  SEM;  $n = 7$  preparations; \* $p < 0.05$  vs. baseline.

RSA component. The hypothesis that the KFn are a major source of excitatory drive for CVMs is anatomically supported by the presence of descending projections targeting the caudal NA (Song et al., 2012; Yokota et al., 2015) and the fact the majority of the FoxP2-expressing neurons that anatomically mark KFn core circuit (Stanic et al., 2018) are glutamatergic (Geerling et al., 2017).

In summary, studies concerned with mediation of RSA suggest that CVMs receive alternating inhibitory and excitatory drives during inspiration and postinspiration to generate RSA. These alternating synaptic drives may predominantly originate from the pre-BötC and KFn respectively. However, the final strength of these anatomically defined synaptic

inputs to CVMs may be further determined by synaptic interactions involving a glycinergic control local inhibitory-excitatory balance with a distributed cardio-respiratory network.

#### 4.2. Role of glycinergic neurotransmission in control of respiration

The organization of fast synaptic neurotransmission between reciprocally connected respiratory neuron populations is the foundation of most contemporary half center oscillator-based models for the generation of three-phase respiratory motor pattern (see Richter, 1982; Rybak et al., 2004 2007; Smith et al., 2007; Shevtsova et al., 2014; Marchenko et al.,

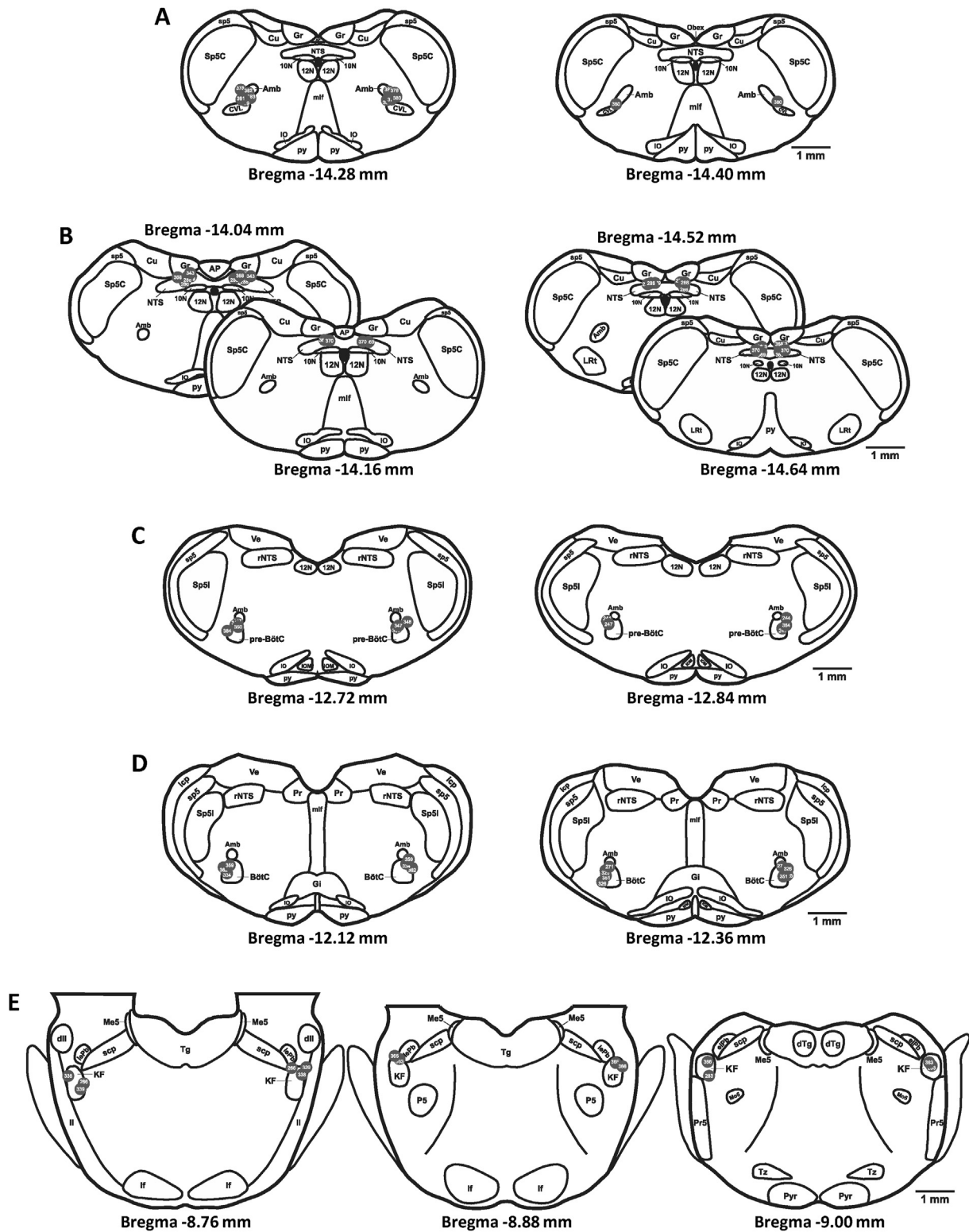


**Fig. 7. Histologic location of the microinjection sites.** Schematic drawings of coronal sections of the brainstem indicating the microinjection sites (grey circles) of strychnine into the NA/CVLM (A), NTS (B), preBötC (C), BötC (D) and KFn (E).

2016). Thus, according to theoretical and computational models mentioned above fast synaptic glycinergic neurotransmission is poised for an important role in generation and timing of respiratory phase oscillations. Experiments using systemic GlyR antagonism in perfused brainstem preparations further promoted this working hypothesis by

causing a shift of the onset of vagal postinspiratory motor bursts from the early expiratory (postinspiratory) phase into inspiration (Busseberg et al., 2001a, 2001b, 2003; Dutschmann and Paton, 2002c; Hayashi and Lipski, 1992; Shevtsova et al., 2014). Moreover, absence of glycinergic inhibition in knock-out mouse models led the animals to premature death

linked to respiratory failure, further underpinning the importance of glycinergic neurotransmission for the generation of eupneic respiration (Busselberg et al., 2001a; Rahman et al., 2015).

The present data demonstrate, for the first time, that glycinergic inhibition is critical for postinspiratory motor pattern formation at the level of the laryngeal motoneurons of the NA. Here local GlyR blockade triggered the shift of the peak postinspiratory motor discharge from early expiration to inspiration. Surprisingly, blocking glycinergic inhibition in designated key nuclei of a distributed ponto-medullary pre-motor network (e.g. NTS, pre-BötC, BötC and KFn) produced neuromodulatory effects like increase in respiratory frequency and phase duration (see Table 1), but did not shift the basic timing of the sequential motor bursting (e.g. shifting postinspiratory activity). Since mono-synaptic projections from the pre-BötC to the overlapping pools of laryngeal motor neurons and CVMs in the NA were recently demonstrated (Menuet et al., 2020) we propose that blocking postsynaptic GlyR of postinspiratory laryngeal adductor motor neurons (LMN) shifts their discharge onset of LMNs to inspiration. Otherwise local disruption of glycinergic neurotransmission did not cause any changes in the burst timing of sequential three-phase motor pattern. In line with results of the present study are observations that glycinergic inhibition is shaping the activity patterns of respiratory motor outputs, but has little role in rhythmogenesis (Janczewski et al., 2013). Furthermore, Janczewski and colleagues showed that blocking glycinergic inhibition has instead profound effects on the mediation of respiratory reflexes such as the inhibitory Hering-Breuer Reflex. A recent study by Flor et al. showed the glycinergic inhibition is involved in the generation of active expiratory motor output in response to sensory stimuli like hypoxia or hypercapnia (Flor et al., 2020). However, the present study was focused on the effect of systemic or local blockade of glycinergic neurotransmission during the stationary generation of respiratory cardio-sympathetic activity pattern and the effects observed after local strychnine microinjections remain underwhelming, compared to what was recently observed with a similar experimental design that investigated the role GABAergic neurotransmission in the same nuclei of the ponto-medullary pre-motor network (Dhingra et al., 2019a, 2019b). Thus, in a broader context, the data of the present study support an alternative model proposed previously by the work of Edward Zuperku and colleagues. This model suggested that an essential GABAergic gain control mechanism shapes the discharge pattern of inspiratory and expiratory neurons types (Krolo et al., 2000; Tonkovic-Capin et al., 2003; Zuperku and McCrimmon, 2002). and not the synaptic oscillation between reciprocally inhibited neuron types. This gain control mechanism matches the conclusion that GABAergic inhibition controls respiratory pattern formation by regulating the balance between excitation and inhibition across the anatomically distributed respiratory network (Dhingra et al., 2019a, 2019b).

#### 4.3. The role of glycinergic inhibition in sympatho-respiratory coupling

The data of the present study suggest that glycinergic neurotransmission is not involved in the timing or respiratory patterning of sympathetic motor activity. Systemic and local strychnine application consistently triggered significant modulations of cardio-respiratory motor activities, but the simultaneously recorded activity of the thoracic sympathetic chain remained unchanged regarding burst timing or discharge amplitudes. The lack of significant effects after local or even systematic blockade of GlyR is surprising, since effective strychnine concentrations should have somehow affected a variety of brainstem nuclei that connect to the sympathetic preganglionic neurons of the intermediolateral cell column of thoracic spinal cord (Jansen et al., 1995). We currently have no sound explanation for this phenomenon, despite that glycinergic inhibition is not involved in the generation or modulation of sympatho-respiratory coupling at stationary network conditions but may come only into play during the processing of sensory information (details see 4.2).

#### 4.4. Conclusion

The data of the present study suggest that glycinergic inhibition at the motoneuronal level is involved in the generation of the inspiratory tachycardia underlying RSA and the separation of inspiratory and postinspiratory bursting of LMNs. Within the distributed ponto-medullary respiratory pre-motor network glycinergic inhibitions is selectively involved in the modulation of the strength of pre-BötC mediated inhibitory drive of CVM and consequently RSA generation. Surprisingly, glycinergic inhibition appears to have no major contribution to respiratory pattern generation or the mediation of respiratory-sympathetic coupling. Therefore, the present study is challenging the common view that reciprocal glycinergic inhibition is an underlying mechanism for the respiratory pattern formation.

#### CRedit authorship contribution statement

**Werner Issao Furuya:** Formal analysis, Data curation, Writing – original draft, Writing – review & editing, conceived and designed the experiments, analyzed the data and prepared figures and tables, conducted all experiments, reviewed drafts of the manuscript, approved the final draft. **Rishi R. Dhingra:** Formal analysis, Data curation, Writing – original draft, Writing – review & editing, conceived and designed the experiments, analyzed the data and prepared figures and tables. **Pedro Trevizan-Baú:** Formal analysis, Data curation, Writing – original draft, Writing – review & editing, contributed to the interpretation of the data. **Robin M. McAllen:** Formal analysis, Data curation, Writing – original draft, Writing – review & editing. **Mathias Dutschmann:** Formal analysis, Data curation, Writing – original draft, Writing – review & editing.

#### Declaration of competing interest

The authors declare that they have no known competing financial interests or personal relationships that could have appeared to influence the work reported in this paper.

#### Acknowledgements

We acknowledge that this work was conducted on the traditional land of the Wurundjeri people of the Kulin nation. We pay our respect to their elders past, present and emerging.

This work was supported by research grants from the National Health and Medical Research Council of Australia (APP1129376); and Australian Research Council (Discovery project DP170104861); PT-B is funded by Melbourne Research Scholarship (University of Melbourne, 181858).

#### Appendix A. Supplementary data

Supplementary data to this article can be found online at <https://doi.org/10.1016/j.crphys.2021.03.001>.

#### References

- Abdala, A.P., Rybak, I.A., Smith, J.C., Zoccal, D.B., Machado, B.H., St-John, W.M., Paton, J.F., 2009. Multiple pontomedullary mechanisms of respiratory rhythmogenesis. *Respir. Physiol. Neurobiol.* 168, 19–25. <https://doi.org/10.1016/j.resp.2009.06.011>.
- Ausborn, J., Koizumi, H., Barnett, W.H., John, T.T., Zhang, R., Molkov, Y.I., Smith, J.C., Rybak, I.A., 2018. Organization of the core respiratory network: insights from optogenetic and modeling studies. *PLoS Comput. Biol.* 14 (4), e1006148 <https://doi.org/10.1371/journal.pcbi.1006148>.
- Adrian, E.D., Bronk, D.W., Phillips, G., 1932. Discharges in mammalian sympathetic nerves. *J. Physiol.* 74, 115–133. <https://doi.org/10.1113/jphysiol.1932.sp002832>.
- Anrep, G.V., Pascual, W., Rösler, R., 1936. Respiratory variations of the heart rate - I—the reflex mechanism of the respiratory arrhythmia. *Proc. R. Soc.* 119, 26. <https://doi.org/10.1098/rspb.1936.0005>.
- Baeke, D.M., Dick, T.E., Paton, J.F., 2008. Pontomedullary transection attenuates central respiratory modulation of sympathetic discharge, heart rate and the baroreceptor reflex in the in situ rat preparation. *Exp. Physiol.* 93, 803–816. <https://doi.org/10.1113/expphysiol.2007.041400>.

- Ben-Tal, A., Shamailov, S.S., Paton, J.F., 2012. Evaluating the physiological significance of respiratory sinus arrhythmia: looking beyond ventilation-perfusion efficiency. *J. Physiol.* 590, 1989–2008. <https://doi.org/10.1113/jphysiol.2011.222422>.
- Bongianni, F., Muto, D., Cinelli, E., Pantaleo, T., 2010. Respiratory responses induced by blockades of GABA and glycine receptors within the Bötzing complex and the pre-Bötzing complex of the rabbit. *Brain Res.* 1344, 134–147. <https://doi.org/10.1016/j.brainres.2010.05.032>.
- Busselberg, D., Bischoff, A.M., Becker, K., Becker, C.M., Richter, D.W., 2001a. The respiratory rhythm in mutant oscillator mice. *Neurosci. Lett.* 316, 99–102. [https://doi.org/10.1016/S0304-3940\(01\)02382-5](https://doi.org/10.1016/S0304-3940(01)02382-5).
- Busselberg, D., Bischoff, A.M., Paton, J.F., Richter, D.W., 2001b. Reorganisation of respiratory network activity after loss of glycinergic inhibition. *Pflügers Archiv* 441, 444–449. <https://doi.org/10.1007/s004240000453>.
- Busselberg, D., Bischoff, A.M., Richter, D.W., 2003. A combined blockade of glycine and calcium-dependent potassium channels abolishes the respiratory rhythm. *Neurosci.* 122, 831–841. <https://doi.org/10.1016/j.neuroscience.2003.07.014>.
- Dhingra, R.R., Dick, T.E., Furuya, W.I., Galan, R.F., Dutschmann, M., 2020. Volumetric mapping of the functional neuroanatomy of the respiratory network in the perfused brainstem preparation of rats. *J. Physiol.* 598, 2061–2079. <https://doi.org/10.1113/JP279605>.
- Dhingra, R.R., Furuya, W.I., Bautista, T.G., Dick, T.E., Galan, R.F., Dutschmann, M., 2019a. Increasing local excitability of brainstem respiratory nuclei reveals a distributed network underlying respiratory motor pattern formation. *Front. Physiol.* 10, 887. <https://doi.org/10.3389/fphys.2019.00887>.
- Dhingra, R.R., Furuya, W.I., Galan, R.F., Dutschmann, M., 2019b. Excitation-inhibition balance regulates the patterning of spinal and cranial inspiratory motor outputs in rats in situ. *Respir. Physiol. Neurobiol.* 266, 95–102. <https://doi.org/10.1016/j.resp.2019.05.001>.
- Dick, T.E., Baekey, D.M., Paton, J.F., Lindsey, B.G., Morris, K.F., 2009. Cardio-respiratory coupling depends on the pons. *Respir. Physiol. Neurobiol.* 168, 76–85. <https://doi.org/10.1016/j.resp.2009.07.009>.
- Dick, T.E., Hsieh, Y.H., Dhingra, R.R., Baekey, D.M., Galan, R.F., Wehrwein, E., Morris, K., 2014. Cardiorespiratory coupling: common rhythms in cardiac, sympathetic, and respiratory activities. *Prog. Brain Res.* 209, 191–205. <https://doi.org/10.1016/B978-0-444-63274-6.00010-2>.
- Dick, T.E., Hsieh, Y.H., Morrison, S., Coles, S.K., Prabhakar, N., 2004. Entrainment pattern between sympathetic and phrenic nerve activities in the Sprague-Dawley rat: hypoxia evoked sympathetic activity during expiration. *Am. J. Physiol. Regul. Integr. Comp. Physiol.* 286. <https://doi.org/10.1152/ajpregu.00485.2003>. R1121–1128.
- Dutschmann, M., Bautista, T.G., Trevizan-Bau, P., Dhingra, R.R., Furuya, W.I., 2021. The pontine Kolliker-Fuse nucleus gates facial, hypoglossal, and vagal upper airway related motor activity. *Respir. Physiol. Neurobiol.* 284, 103563. <https://doi.org/10.1016/j.resp.2020.103563>.
- Dutschmann, M., Herbert, H., 2006. The Kolliker-Fuse nucleus gates the postinspiratory phase of the respiratory cycle to control inspiratory off-switch and upper airway resistance in rat. *Eur. J. Neurosci.* 24, 1071–1084. <https://doi.org/10.1111/j.1460-9568.2006.04981.x>.
- Dutschmann, M., Paton, J.F., 2002a. Glycinergic inhibition is essential for co-ordinating cranial and spinal respiratory motor outputs in the neonatal rat. *J. Physiol.* 543, 643–653. <https://doi.org/10.1113/jphysiol.2001.013466>.
- Dutschmann, M., Paton, J.F., 2002b. Inhibitory synaptic mechanisms regulating upper airway patency. *Respir. Physiol. Neurobiol.* 131, 57–63. [https://doi.org/10.1016/S1569-9048\(02\)00037-x](https://doi.org/10.1016/S1569-9048(02)00037-x).
- Dutschmann, M., Paton, J.F., 2002c. Trigeminal reflex regulation of the glottis depends on central glycinergic inhibition in the rat. *Pflügers Archiv* 282, R999–R1005. <https://doi.org/10.1152/ajpregu.00502.2001>.
- Dutschmann, M., Wilson, R.J., Paton, J.F., 2000. Respiratory activity in neonatal rats. *Auton. Neurosci.* 84, 19–29. [https://doi.org/10.1016/S1566-0702\(00\)00177-6](https://doi.org/10.1016/S1566-0702(00)00177-6).
- Ezure, K., Tanaka, I., Kondo, M., 2003. Glycine is used as a transmitter by decrementing expiratory neurons of the ventrolateral medulla in the rat. *J. Neurosci.* 23, 8941–8948. <https://doi.org/10.1523/JNEUROSCI.23-26-08941.2003>.
- Farmer, D.G., Dutschmann, M., Paton, J.F., Pickering, A.E., McAllen, R.M., 2016. Brainstem sources of cardiac vagal tone and respiratory sinus arrhythmia. *J. Physiol.* 594, 7249–7265. <https://doi.org/10.1113/JP273164>.
- Feldman, J.L., Del Negro, C.A., 2006. Looking for inspiration: new perspectives on respiratory rhythm. *Nat. Rev. Neurosci.* 7, 232–242. <https://doi.org/10.1038/nrn1871>.
- Flor, K.C., Barnett, W.H., Karlen-Amarante, M., Molkov, Y.I., Zoccal, D.B., 2020. Inhibitory control of active expiration by the Bötzing complex in rats. *J. Physiol.* 598, 4969–4994. <https://doi.org/10.1113/JP280466>.
- Geerling, J.C., Yokota, S., Rukhadze, I., Roe, D., Chamberlin, N.L., 2017. Kolliker-Fuse GABAergic and glutamatergic neurons project to distinct targets. *J. Comp. Neurol.* 525, 1844–1860. <https://doi.org/10.1002/cne.24164>.
- Gilbey, M.P., 2007. Sympathetic rhythms and nervous integration. *Clin. Exp. Pharmacol. Physiol.* 34, 356–361. <https://doi.org/10.1111/j.1440-1681.2007.04587.x>.
- Gilbey, M.P., Jordan, D., Richter, D.W., Spyer, K.M., 1984. Synaptic mechanisms involved in the inspiratory modulation of vagal cardio-inhibitory neurones in the cat. *J. Physiol.* 356, 65–78. <https://doi.org/10.1113/jphysiol.1984.sp015453>.
- Gomez, J., Hülsmann, S., Ohno, K., Eulenburg, V., Szöke, K., Richter, D., Betz, H., 2003. Inactivation of the glycine transporter 1 gene discloses vital role of glial glycine uptake in glycinergic inhibition. *Neuron* 40 (4), 785–796. [https://doi.org/10.1016/S0896-6273\(03\)00672-x](https://doi.org/10.1016/S0896-6273(03)00672-x).
- Hayano, J., Yasuma, F., Okada, A., Mukai, S., Fujinami, T., 1996. Respiratory sinus arrhythmia. A phenomenon improving pulmonary gas exchange and circulatory efficiency. *Circulation* 94, 842–847. <https://doi.org/10.1161/01.cir.94.4.842>.
- Hayashi, F., Lipski, J., 1992. The role of inhibitory amino acids in control of respiratory motor output in an arterially perfused rat. *Respir. Physiol.* 89, 47–63. [https://doi.org/10.1016/0034-5687\(92\)90070-d](https://doi.org/10.1016/0034-5687(92)90070-d).
- Iriuchijima, J., Kumada, M., 1964. Activity of single vagal fibers efferent to the heart. *Jpn. J. Physiol.* 14, 479–487. <https://doi.org/10.2170/jjphysiol.14.479>.
- Janczewski, W.A., Tashima, A., Hsu, P., Cui, Y., Feldman, J.L., 2013. Role of inhibition in respiratory pattern generation. *J. Neurosci.* 33 (13), 5454–5465. <https://doi.org/10.1523/JNEUROSCI.1595-12.2013>.
- Jansen, A.S., Wessendorf, M.W., Loewy, A.D., 1995. Transneuronal labeling of CNS neuropeptide and monoamine neurons after pseudorabies virus injections into the stellate ganglion. *Brain Res.* 683, 1–24. [https://doi.org/10.1016/0006-8993\(95\)00276-v](https://doi.org/10.1016/0006-8993(95)00276-v).
- Jones, S.E., Dutschmann, M., 2016. Testing the hypothesis of neurodegeneracy in respiratory network function with a priori transected arterially perfused brain stem preparation of rat. *J. Neurophysiol.* 115, 2593–2607. <https://doi.org/10.1152/jn.01073.2015>.
- Krolo, M., Stuth, E.A., Tonkovic-Capin, M., Hopp, F.A., McCrimmon, D.R., Zuperku, E.J., 2000. Relative magnitude of tonic and phasic synaptic excitation of medullary inspiratory neurons in dogs. *Am. J. Physiol. Regul. Integr. Comp. Physiol.* 279, R639–R649. <https://doi.org/10.1152/ajpregu.2000.279.2.R639>.
- Kunze, D.L., 1972. Reflex discharge patterns of cardiac vagal efferent fibres. *J. Physiol.* 222, 1–15. <https://doi.org/10.1113/jphysiol.1972.sp009784>.
- Manzke, T., Niebert, M., Koch, U.R., Caley, A., Vogelgesang, S., Hülsmann, S., Ponimaskin, E., Müller, U., Smart, T.G., Harvey, R.J., Richter, D.W., 2010. Serotonin receptor 1A-breathing phosphorylation of glycine receptor alpha3 controls breathing in mice. *J. Clin. Invest.* 120, 4118–4128. <https://doi.org/10.1172/JCI43029>.
- Marchenko, V., Koizumi, H., Mosher, B., Koshiya, N., Tariq, M.F., Bezdudnaya, T.G., Zhang, R., Molkov, Y.I., Rybak, I.A., Smith, J.C., 2016. Perturbations of respiratory rhythm and pattern by disrupting synaptic inhibition within pre-bötzing and botzinger complexes. *eNeuro* 3 (2). <https://doi.org/10.1523/ENEURO.0011-16.2016>.
- McAllen, R.M., Spyer, K.M., 1978. Two types of vagal preganglionic motoneurons projecting to the heart and lungs. *J. Physiol.* 282, 353–364. <https://doi.org/10.1113/jphysiol.1978.sp012468>.
- Menuet, C., Connelly, A.A., Bassi, J.K., Melo, M.R., Le, S., Kamar, J., Kumar, N.N., McDougall, S.J., McMullan, S., Allen, A.M., 2020. PreBötzing complex neurons drive respiratory modulation of blood pressure and heart rate. *Elife* 9. <https://doi.org/10.7554/eLife.57288>.
- Morgado-Valle, C., Baca, S.M., Feldman, J.L., 2010. Glycinergic pacemaker neurons in preBötzing complex of neonatal mouse. *J. Neurosci.* 30, 3634–3639. <https://doi.org/10.1523/JNEUROSCI.3040-09.2010>.
- Paton, J.F., 1996. A working heart-brainstem preparation of the mouse. *J. Neurosci. Methods* 65, 63–68. [https://doi.org/10.1016/0165-0270\(95\)00147-6](https://doi.org/10.1016/0165-0270(95)00147-6).
- Pickering, A.E., Paton, J.F., 2006. A decerebrate, artificially-perfused in situ preparation of rat: utility for the study of autonomic and nociceptive processing. *J. Neurosci. Methods* 155, 260–271. <https://doi.org/10.1016/j.jneumeth.2006.01.011>.
- Pilowsky, P., 1995. Good vibrations? Respiratory rhythms in the central control of blood pressure. *Clin. Exp. Pharmacol. Physiol.* 22, 594–604. <https://doi.org/10.1111/j.1440-1681.1995.tb02072.x>.
- Rahman, J., Besser, S., Schnell, C., Eulenburg, V., Hirrlinger, J., Wojcik, S.M., Hülsmann, S., 2015. Genetic ablation of VIAAT in glycinergic neurons causes a severe respiratory phenotype and perinatal death. *Brain Struct. Funct.* 220, 2835–2849. <https://doi.org/10.1007/s00429-014-0829-2>.
- Richter, D.W., 1982. Generation and maintenance of the respiratory rhythm. *J. Exp. Biol.* 100, 93–107.
- Richter, D.W., Spyer, K.M., 1990. *Cardiorespiratory control. In: Central Regulation of Autonomic Functions.* Oxford University Press, pp. 189–217.
- Richter, D.W., Smith, J.C., 2014. Respiratory rhythm generation in vivo. *Physiology* 29 (1), v58–71. <https://doi.org/10.1152/physiol.00035.2013>. PMID: 24382872; PMCID: PMC3929116.
- Rybak, I.A., Shevtsova, N.A., Paton, J.F., Dick, T.E., St-John, W.M., Morschel, M., Dutschmann, M., 2004. Modeling the ponto-medullary respiratory network. *Respir. Physiol. Neurobiol.* 143, 307–319. <https://doi.org/10.1016/j.resp.2004.03.020>.
- Rybak, I.A., Abdala, A.P., Markin, S.N., Paton, J.F., Smith, J.C., 2007. Spatial organization and state-dependent mechanisms for respiratory rhythm and pattern generation. *Prog. Brain Res.* 165, 201–220. [https://doi.org/10.1016/S0079-6123\(06\)65013-9](https://doi.org/10.1016/S0079-6123(06)65013-9).
- Sharp, D.B., Wang, X., Mendelowitz, D., 2014. Dexmedetomidine decreases inhibitory but not excitatory neurotransmission to cardiac vagal neurons in the nucleus ambiguus. *Brain Res.* 1574, 1–5. <https://doi.org/10.1016/j.brainres.2014.06.010>.
- Shevtsova, N.A., Busselberg, D., Molkov, Y.I., Bischoff, A.M., Smith, J.C., Richter, D.W., Rybak, I.A., 2014. Effects of glycinergic inhibition failure on respiratory rhythm and pattern generation. *Prog. Brain Res.* 209, 25–38. <https://doi.org/10.1016/B978-0-444-63274-6.00002-3>.
- Smith, J.C., Abdala, A.P., Koizumi, H., Rybak, I.A., Paton, J.F., 2007. Spatial and functional architecture of the mammalian brain stem respiratory network: a hierarchy of three oscillatory mechanisms. *J. Neurophysiol.* 98, 3370–3387. <https://doi.org/10.1152/jn.00985.2007>.
- Smith, J.C., Ellenberger, H.H., Ballanyi, K., Richter, D.W., Feldman, J.L., 1991. Pre-Bötzing complex: a brainstem region that may generate respiratory rhythm in mammals. *Science* 254, 726–729. <https://doi.org/10.1126/science.1683005>.
- Song, G., Wang, H., Xu, H., Poon, C.S., 2012. Kolliker-Fuse neurons send collateral projections to multiple hypoxia-activated and nonactivated structures in rat brainstem and spinal cord. *Brain Struct. Funct.* 217, 835–858. <https://doi.org/10.1007/s00429-012-0384-7>.

- Stanic, D., Dhingra, R.R., Dutschmann, M., 2018. Expression of the transcription factor FOXP2 in brainstem respiratory circuits of adult rat is restricted to upper-airway premotor areas. *Respir. Physiol. Neurobiol.* 250, 14–18. <https://doi.org/10.1016/j.resp.2018.01.014>.
- Tonkovic-Capin, V., Stucke, A.G., Stuth, E.A., Tonkovic-Capin, M., Hopp, F.A., McCrimmon, D.R., Zuperku, E.J., 2003. Differential processing of excitation by GABAergic gain modulation in canine caudal ventral respiratory group neurons. *J. Neurophysiol.* 89, 862–870. <https://doi.org/10.1152/jn.00761.2002>.
- Winter, S.M., Fresemann, J., Schnell, C., Oku, Y., Hirrlinger, J., Hulsman, S., 2009. Glycinergic interneurons are functionally integrated into the inspiratory network of mouse medullary slices. *Pflügers Archiv* 458, 459–469. <https://doi.org/10.1007/s00424-009-0647-1>.
- Yokota, S., Kaur, S., VanderHorst, V.G., Saper, C.B., Chamberlin, N.L., 2015. Respiratory-related outputs of glutamatergic, hypercapnia-responsive parabrachial neurons in mice. *J. Comp. Neurol.* 523, 907–920. <https://doi.org/10.1002/cne.23720>.
- Zafra, F., Aragon, C., Olivares, L., Danbolt, N.C., Gimenez, C., Storm-Mathisen, J., 1995. Glycine transporters are differentially expressed among CNS cells. *J. Neurosci.* 15, 3952–3969. <https://doi.org/10.1523/JNEUROSCI.15-05-03952.1995>.
- Zuperku, E.J., McCrimmon, D.R., 2002. Gain modulation of respiratory neurons. *Respir. Physiol. Neurobiol.* 168, 19–25. [https://doi.org/10.1016/s1569-9048\(02\)00042-3](https://doi.org/10.1016/s1569-9048(02)00042-3).